Developing a hybrid wind instrument: using a loudspeaker to couple a theoretical exciter to a real resonator

K. Buys, D. Sharp and R. Laney
Open University, Walton Hall, MK7 6A Milton Keynes, Buckinghamshire, UK
kurijn.buys@open.ac.uk

A hybrid wind instrument generates self-sustained sounds via a real-time interaction between a computed physical model of an exciter (such as human lips interacting with a mouthpiece) and a real acoustic resonator. Successful implementation of a hybrid wind instrument will not only open up new musical possibilities but will also provide a valuable research tool. However, attempts to produce a hybrid instrument have so far fallen short, in terms of both the accuracy and the variation in the sound produced. The principal reason for the failings of previous hybrid instruments is the actuator which, controlled by the physical model of the exciter, introduces a fluctuating component into the air flow injected into the resonator. In the present paper, the possibility of using a loudspeaker to supply the calculated excitation signal is explored. A theoretical study using established physical models is carried out, yielding useful rules for choosing the best loudspeaker for a given resonator. Acoustical coupling and feedback stability are considered. Experimental studies are reported which provide the loudspeaker's "electrical input to dynamic volume flow rate" transfer function. Simulations of the entire system, along with initial experimental investigations, confirm a coherent self-sustained operation.

1   Introduction

The concept of hybrid wind instrumentation is explained in figure 1: a physical model of a mouthpiece (including the player's mouth) is simulated on a computer and interacts with a real acoustical resonator so that the whole is able to generate hybrid self-sustained sounds.

Such a device promotes two main research interests. First,
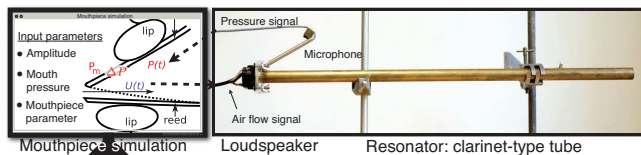
Figure 1: The hybrid wind instrument set-up: a computed mouthpiece in interation with a physical resonator by means of a loudspeaker.

placing it in the context of acoustic wind instrument research, it would be of substantial value to have a repeatable and precisely quantified control over an exciter that is linked to a resonator of interest. This matches with the objectives of the now classical "artificial mouths" for wind instruments [1, 2]. The opposite concept is also of interest: studying how the excitation relates to the produced sound, by comparison with real and simulated wind instruments and wind instrument theories [3].

A second interest is the exploration of the device's potential as a musical instrument, lying mostly in the timbre domain, which is an active musical composition focus of today [4, 5]. Here, the same control precision can play a role in the accessibility of certain (variations of) sounds. While, the computed environment allows modelling any conceivable excitation and handles electronic parameter variations, the physical control over the resonator (the fingering) remains, which opens up an alternative range of musical expression with the advantage of relatively low computational power needs. Only minor contributions on this particular concept have been made to date. Maganza first briefly explored a set-up [6] and since then a small number of works on closely related subjects have been carried out, for example [7, 8]. More recently, an identical approach has been implemented, but using an electrovalve as flow actuator [9].

An important conclusion of these studies is that the actuator, which is the component that translates the computed flow rate output into a real acoustical flow, has been the main reason for low accuracy.

In the present study, the idea of using a loudspeaker to perform the actuation is investigated. While this transducer is not capable of generating a mean flow, that flow component is known to be unimportant for proper self-sustained functioning [3]. Figure 2 represents the global flow chart of a fully functioning hybrid instrument. We will refer to this chart throughout the paper.
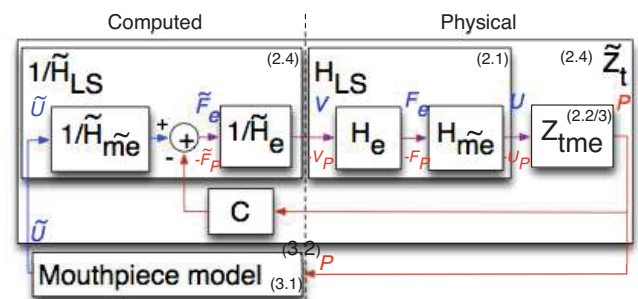
Figure 2: Flow chart of the hybrid instrument's computed and physical parts. The corresponding sections are indicated between brackets.

2   The loudspeaker-tube system

Preliminary work has been carried out to investigate the behavior of a loudspeaker mounted on a "clarinet-type" tube. As the loudspeaker doesn't provide an ideal rigid termination to the tube, the input impedance deviates from that for a classic closed-open cylinder. Therefore coupled physical models of the loudspeaker and tube are considered (as represented in figure 3, explained later). Also, measurements are performed to find the absolute parameter values that are used both to predict a calibrated "flow rate response" for the loudspeaker and to undo the coupling. We
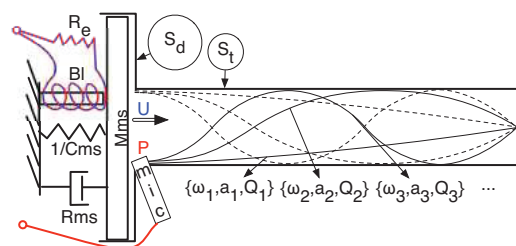
Figure 3: Outline of the assembled loudspeaker and tube models.

assume that the sound propagates as plane waves, which is valid in such small sections for the frequency range of consideration [3]. As the volume between the loudspeaker diaphragm and the tube is small, the change in section size

between the loudspeaker (with diaphragm section S_d) and the tube (with section S_t) has negligible influence on both the "volume flow rate" U and the pressure P, so that they can be considered as equal in both places. We note that we will express all equations in the complex s-domain by using the Laplace Transform, with $s = j\omega$, $\omega = 2\pi f$ and f the frequency in Hz.

2.1 The loudspeaker

The use of a loudspeaker as a "flow generating" device requires a study of this actuator. Ideally, a flow rate signal calculated by the mouthpiece model should proportionally and directly be converted into a physical flow by the actuator, which means that we need to know the loudspeaker's transfer function.

We adopted a classical model, initially proposed by Small [10]. It consists of an electrical part with R_e and L_e, respectively the DC resistance and the inductance of the voice coil, with input voltage V. The mechanical part is modelled by a 1-DOF mass-spring-damper system, with the conventional parameter names Mms, Cms and Rms respectively the mass, inverse spring stiffness and damping coefficient, and receives a force F_e from the voice-coil. The approximate mechanical impedance for this loudspeaker model can be written as:

$$Z_{\widetilde{me}} = \frac{Mms(\omega_s^2 + \frac{\omega_s s}{Qts} + s^2)}{s},$$ (1)

with $\omega_s = \sqrt{Mms\,Cms}$, the speaker's resonant frequency and $Qts = \frac{\sqrt{Mms/Cms}}{Rts(Rms,L_e,R_e)}$ and Rts the total quality factor and damping coefficient. The transfer functions for the electrical (H_e) and mechanical ($H_{\widetilde{me}}$) loudspeaker parts (see figure 2) are expressed by the ratios of outgoing over incoming signals:

$$H_e = \frac{F_e(s)}{V(s)} = \frac{Bl}{R_e + s\,L_e},$$ (2)

with Bl, a coil factor, and:

$$H_{\widetilde{me}} = \frac{U(s)}{F_e(s)} = \frac{S_d}{Z_{\widetilde{me}}},$$ (3)

where U is the outputted volume flow rate and S_d is the diaphragm surface area. The complete loudspeaker system can then be represented by an overall transfer function that expresses the volume flow rate per input voltage:

$$H_{LS} = \frac{U(s)}{V(s)} = H_e\,H_{\widetilde{me}}.$$ (4)

We used a traditional method [10] and a method proposed by Klippel [11] to carry out measurements on a 1" Tang Band loudspeaker of type W1-1070SE. Figure 4 shows the measurement of the output membrane velocity over the input voltage and the resulting least-square regression using $H_e/Z_{\widetilde{me}}$. The regression allowed to obtain the parameters presented in table 1. We note that the observed phase lag increases more and more with frequency and can not be taken into account by our model.

2.2 The resonator

The resonator employed in our hybrid instrument is a tube whose dimensions roughly match those of a soprano
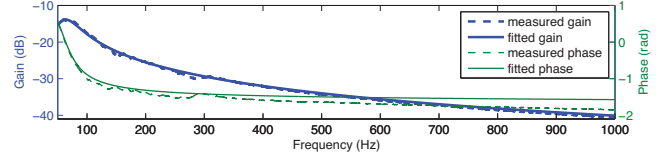
Figure 4: Measured and fitted transfer function curves for H_e/Z_{me}.

Table 1: The obtained estimated loudspeaker parameters.

R_e	$6.21\,\Omega$	ω_s	$2\pi \times 63.7\,\text{rad s}^{-1}$
Bl	$3.36\,\text{T m}$	Mms	$9.11 \times 10^{-3}\,\text{kg}$
Qts	1.34	Cms	$6.84 \times 10^{-4}\,\text{m N}^{-1}$
		S_d	$8.04 \times 10^{-4}\,\text{m}^2$

clarinet playing its lowest note. The inner diameter measures 14.2 mm and its length is 58 cm.

Although a resonator model is not directly needed for a real hybrid instrument, we include this study to both analyse the impact of the coupling with the loudspeaker and to be able to compare the hybrid sounds with "entirely simulated" sounds, i.e. where the resonator is also simulated. We use a resonator model based on a modal decomposition of the input impedance that describes each impedance peak as a second order transfer function with real coefficients [12]:

$$Z_t(s) = Z_c \sum_{n=1}^{N} \frac{a_n s}{\omega_n^2 + \frac{\omega_n}{Q_n}s + s^2},$$ (5)

where $\{a_n, \omega_n, Q_n\}$ are the real modal coefficients: the amplitude, resonance frequency and quality factor of mode n, and $Z_c = \frac{\rho c}{S_t}$ is the characteristic impedance of the resonator, with ρ the density of air, c the speed of sound and S_t the cross-sectional area of the tube. This technique allows approximation of a finite number of modes of the measured impedance with a good precision.

The modal coefficients are found using an iterative least square fitting method, using eq. (5), on a complex impedance curve measured with the "capillary tube method" [13]. Figure 5 shows the modal approximated impedance curve around the resonant frequencies (in solid green). This curve is found from the measured curve (not plotted) with a ± 2 cent precision for the resonance frequencies and a ± 0.3 dB precision in a large range around the resonances.

2.3 Coupled tube and loudspeaker

To model a loudspeaker that is coupled to a tube, we can simply combine the analogous loudspeaker circuit with an analogous circuit for the tube based on the modal decomposition (represented in figure 6). Following the analogy of voltage representing the pressure, the coupling is represented by a transformer, relating the force F_P and velocity v of the loudspeaker membrane respectively to the pressure P and the flow rate at the instrument entrance U by: $F_P = S_d P$ and $v\,S_d = U$. The coupled tube impedance can be calculated by:

$$Z_{t\widetilde{me}}(s) = \left(\frac{1}{Z_t} + \frac{S_d^2}{Z_{\widetilde{me}}}\right)^{-1}.$$ (6)

Given that the modes are relatively widely spaced in frequency, we may assume that the coupling with the
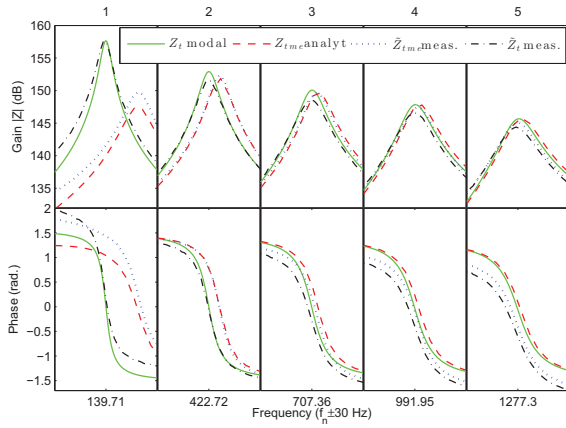
Figure 5: Modal, analytic coupled, measured coupled and measured uncoupled tube impedance curves ±30 Hz around the five first modes.
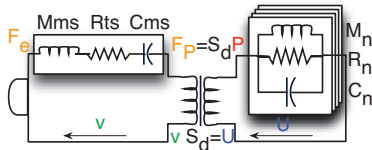
Figure 6: Equivalent electronic circuit representing the loudspeaker's mechanical part coupled with the modal tube impedance.

loudspeaker occurs independently for each mode n. The new resonant frequency $\omega_{n\widetilde{me}}$ for mode n is found from the roots of the imaginary part of $Z_{t\widetilde{me}}$. Considering equations (6), (1) and (5) for a single mode, it can be showed that this results in:

$$-(\omega_n^2 + s^2)(\omega_s^2 + s^2) = \omega_{cn}^2 \, s^2, \qquad (7)$$

with $\omega_{cn} = \sqrt{\frac{Z_c S_d^2 a_n}{Mms}}$, the "coupling frequency" (we note that the variation between the a_n is small). This expression can be interpreted as a second order function whose roots directly lead to (for $\omega_n \gg \omega_s$):

$$\omega_{n\widetilde{me}} = \omega_n \sqrt{1 + \frac{\omega_{cn}^2}{\omega_n^2}}, \qquad (8)$$

which shows that the strongest coupling occurs for the first mode. For our loudspeaker we have $\omega_{c1} = 2\pi \times 73.6\,\mathrm{rad\,s^{-1}}$ so that the first tube resonance $\omega_1 = 2\pi \times 139.7\,\mathrm{rad\,s^{-1}}$ shifts to $\omega_{1\widetilde{me}} = 2\pi \times 157.8\,\mathrm{rad\,s^{-1}}$. This shift can easily become much larger for the same tube and a loudspeaker with a greater $\frac{S_d^2}{Mms}$ factor. A similar development can be followed to find a loudspeaker-coupled Q-factor:

$$\frac{1}{Q_{n\widetilde{me}}} = \frac{1}{Q_n}\left(1 + \frac{\omega_{cn}^2 \omega_s Q_n}{\omega_{n\widetilde{me}}^2 \omega_n Qts}\right). \qquad (9)$$

Here, a higher ω_{cn} has a significantly stronger influence. For our case, the ratio of Q shifting is $\frac{Q_{n\widetilde{me}}}{Q_n} = 0.33$, but for a similar loudspeaker, with a 2" diaphragm for instance, that ratio already becomes ten times smaller.
The resulting coupled tube impedance, as calculated by equation (6), is presented in figure 5 (in dashed red). A modal calculation by inserting the coupled tube parameters $a_{n\widetilde{me}}$ and $Q_{n\widetilde{me}}$ in equation (5) resulted in a close match (not plotted).

2.4 Accounting for the loudspeaker

For coherent functioning of the hybrid instrument, the calculated flow rate signal by the mouthpiece model $\widetilde{U}$ should be acoustically reproduced by the loudspeaker: U. Therefore, two filters are considered: one to flatten the loudspeaker response and another to account for the coupling with the tube. These filters are executed by the real-time computing system that is described in appendix A. We note that the responses of both the power amplifier and the microphone have a negligible influence and hence are not taken into account in our study. For an optimal dynamic range, a 0.23 V chirp signal is used for all measurements.

2.4.1 Accounting for the loudspeaker response

Assuming the loudspeaker is not coupled with the tube, the feedforward filter that would undo its response would simply be the inverse of the loudspeaker transfer function (4). The problem is that this represents a non-causal filter, which evidently can not be executed in real-time. Therefore, a loudspeaker is chosen that has a resonant frequency far enough below the playing frequencies, so that only the first order (Mms) term is of importance. Hence, the approximated inverse transfer function can be written as:

$$\widetilde{H}_{LS}^{-1} = \widetilde{H}_{\widetilde{me}}^{-1}\,\widetilde{H}_e^{-1}, \qquad (10)$$

with:

$$\widetilde{H}_{\widetilde{me}}^{-1} = \frac{\widetilde{F}_e(z)}{\widetilde{U}(z)} = \frac{Mms\,(z-1)}{S_d\,T_s\,z} \approx \frac{Mms\,s}{S_d}, \qquad (11)$$

where the continuous derivative s is approximated by a discrete transfer function (with z the discrete equivalent of s and T_s, the sample time) that can be executed by the computer. The inductance in the electrical part is also negligible at low frequencies (less than a few kHz), so that:

$$\widetilde{H}_e^{-1} = \frac{V(z)}{\widetilde{F}_e(z)} = \frac{R_e}{Bl}. \qquad (12)$$

The implementation in the whole system is depicted in figure 2. By applying the filters to the loudspeaker-tube system, and measuring the pressure with the microphone, a hybrid tube impedance can be determined:

$$\widetilde{Z}_{t\widetilde{me}} = \frac{P}{\widetilde{U}} = \widetilde{H}_{LS}^{-1} H_{LS} Z_{tme}. \qquad (13)$$

This "virtual" tube impedance still contains the loudspeaker-tube coupling, which is dealt with in the next section. The measured result is also plotted (in dotted blue) in figure 5. While close to the analytical coupled curve, the first mode is slightly increased in amplitude due to the first order approximation of the loudspeaker. The increasing phase shift at higher frequencies can be explained by the phase-lag problem mentioned in section 2.1.

2.4.2 Accounting for the the loudspeaker-tube coupling

The principle behind the feedback filter that accounts for the coupling between the loudspeaker and tube is very simple and is based on Newton's third law: in order to undo the force on the loudspeaker diaphragm due to the pressure in front of it, $S_d\,P$, it is necessary to add its inverse to F_e. As P is

directly measured by the microphone and F_e can be accessed by using $\widetilde{H}_e^{-1}$, the feedback controller is simply

$$C = -S_d. \tag{14}$$

This proportional controller solution can also be found by applying basic feedback control theory. The implementation of the control loop is also depicted in the global flow chart in figure 2. Since the mechanical part of the loudspeaker doesn't come into play here, there is practically no approximation issue. The resulting "restored" impedance curve $\widetilde{Z}_t$ is also plotted (in black dash-dotted) in figure 5. The same deviations as the measured $Z_{t\widetilde{me}}$ are still visible, but the result is fairly close to the original measured and modally approximated tube impedance Z_t.

3 Hybrid functionality

As the tube impedance $\widetilde{Z}_t$ is the ratio of pressure P and flow rate $\widetilde{U}$, both accessible by the computer, it is possible to supply any excitation to allow hybrid self-sustained sounds. In this first investigation, we chose a well-established single-reed mouthpiece model as the exciter.
A low-pass filter was added after the microphone input with a cut-off at 6 kHz, to prevent erroneous feedback (possibly due to the plane-wave approximation becoming invalid).

3.1 Single-reed mouthpiece model

For the mouthpiece, the classical quasi-static (i.e. the reed dynamics are neglected) model depicted in figure 7 was adopted [1, 9]. The displacement Y of the reed (with
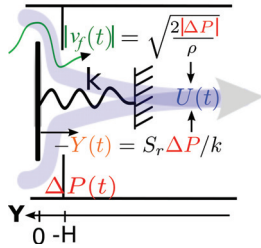
Figure 7: The quasi-static mouthpiece model.

stiffness k_r) is created by the pressure difference between mouth and mouthpiece interior ($P_m - P$), acting on part of the reed surface S_r:

$$Y = \frac{-S_r(P_m - P)}{k_r}. \tag{15}$$

The air flow that enters the instrument can be expressed as the product of the flow velocity v_f and the effective reed opening section S_f. The former can be found by the Bernoulli theorem applied between the mouth and the reed flow channel (thus between the mentioned pressure difference) and the latter is assumed to be linearly related to the reed displacement [3]:

$$U = \underbrace{sign(P_m - P) \sqrt{\frac{2|P_m - P|}{\rho}}}_{v_f} \underbrace{\mathcal{H}(Y + H)(Y + H)w}_{S_f}, \tag{16}$$

where ρ is the air density and w is the effective reed width. The *sign* operator is introduced to make the calculation of

negative flows possible and the Heaviside function $\mathcal{H}$ to hold a zero flow rate when the reed hits the lay, which occurs above the "beating pressure" P_M.
This equation can be simplified and normalized (or "nondimensionalized") by defining $p = \frac{P}{P_M}$, $u = \frac{U\,\zeta\,P_M}{Z_c}$ (where ζ lumps all mouthpiece parameters together) and $\gamma = \frac{P_m}{P_M}$:

$$u = sign(\gamma - p) \sqrt{|\gamma - p|}\,\mathcal{H}(p - \gamma + 1)(p - \gamma + 1). \tag{17}$$

There are three remaining independent parameters: P_M, which determines the signal amplitude (without timbre variation for a linear resonator), the mouth pressure γ and the mouthpiece parameter ζ, which both have an effect on the signal shape and attack, and thus the timbre of the sound [14].

3.2 Hybrid versus simulated instruments

We performed a preliminary evaluation of the hybrid self-sustained operation by combining the previously described loudspeaker-tube system with the filters to account for the loudspeaker response and loudspeaker tube coupling and with the computed mouthpiece model. We varied the normalized mouth pressure γ from 0.33 to 2.1 for six values of ζ (between 0.1 and 0.35) and observed the mean (RMS) normalized pressure and the spectral centroid of p. Both of these features are known to vary as a function of the mouthpiece parameters and the former has been analytically studied [15]. The results are plotted in figure 8, along with a simulation of the entire instrument, which includes a tube simulation where the loudspeaker is assumed to be a rigid piston with an ideal response. While a beating pressure
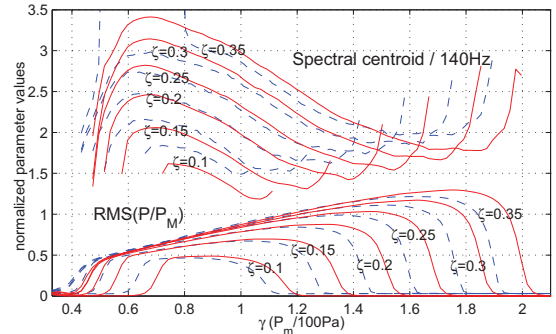
Figure 8: RMS and spectral centroid evolutions of the pressure signal for several ζ and (increasing) γ values; for hybrid (dashed blue) and simulated instruments (solid red).

of $P_M = 100$ Pa is set, we found closely matching hybrid results (for the simulation these curves are invariant) for P_M from 50 Pa to 400 Pa.
This result is a first indication of a fairly coherent performance of the hybrid instrument, which also corresponds to findings in literature [15]. Any hypothesis for the reasons of the variation between the hybrid and entire simulations are not made yet, but it is interesting to note that the oscillation threshold can be as low as $\gamma_{th} = 0.34$. For $\zeta \geq 0.35$ and $\gamma \approx 0.7 \pm 0.2$, an unstable state is easily encountered. Closer signal observations indicate that this occurs when the reed is in fully opened position during self-sustained operation, where a steep flow-rate variation applies for small pressure variations. The high-valued

spectral centroid around this zone might be a good indicator for this issue. Additional measurements further proved a very good repeatability.

4 Conclusions and perspectives

The development of a hybrid wind instrument, by means of a loudspeaker has been successfully implemented in theory and practice.

In the first instance, we found that the (undesired) coupling between the loudspeaker and the resonator, in terms of resonance frequency and quality-factor shifting of the latter, rapidly increases for a higher coupling frequency $\omega_{cn} = \sqrt{\frac{Z_c S_d^2 a_n}{Mms}}$. This demonstrated the value of using a small-diaphragm loudspeaker.

In a next computational stage, we derived a filter to remove the response of the loudspeaker and a feedback filter to undo the coupling. The measured results are close to the theory and the foremost differences are identified by the approximations made. All findings provided information regarding which loudspeaker would be an optimal choice for a hybrid construction.

Finally, a hybrid self-sustained operation has been demonstrated (in reasonable accordance with reported theories and with an entire simulation of the wind instrument) and a coherent dynamic range has been found for P_M = 50 Pa to 400 Pa.

While a subsequent in-depth experimental investigation will allow for a more precise qualitative assessment, this work shows the suitability of using a loudspeaker as the actuator for hybrid wind instrumentation that can serve to answer questions in both acoustical wind research and in musical research contexts.

Acknowledgments

References

[1] T. A. Wilson and G. S. Beavers, "Operating modes of the clarinet," *J. Acoust. Soc. Am.*, vol. 56, pp. 653–658, 1974.

[2] D. Ferrand and C. Vergez, "Blowing machine for wind musical instrument : toward a real-time control of the blowing pressure," *2008 16th Mediterr. Conf. Control Autom.*, 2008.

[3] A. Hirschberg, "Aero-acoustics of wind instruments," in *Mech. Music. Instruments* (A. Hirschberg J. Kergomard and G. Weinreich, eds.), Wien: Springer, 1995.

[4] P. Boulez, "Timbre and composition - timbre and language," *Contemp. Music Rev.*, vol. 2, part. 1, p. 169, 1987.

[5] N. Farwell, *Being what I Am: Doing what I Do; Manifesto of a Composer*. PhD thesis, University of East Anglia, Norwich, UK, 2001.

[6] C. Maganza, *Excitations non linéaire d'un conduit acoustique cylindrique. Observations de doublements de période précédant un comportant chaotique. Application à la Clarinette*. PhD thesis, Université du Maine, 1985.

[7] J. Guérard, *Modélisation numérique et simulation expérimentale de systèmes acoustiques - Application aux instruments de musique*. PhD thesis, Université Paris 6, 1998.

[8] N. Grand, *Etude du seuil d'oscillation des systèmes acoustiques non-linéaires de type instrument à vent*. PhD thesis, Université Paris 7, 1994.

[9] K. Buys and C. Vergez, "A hybrid reed instrument: an acoustical resonator with a numerically simulated mouthpiece," in *Proc. Acoust. 2012*, (Nantes), 2012.

[10] R. H. Small, "Direct Radiator Loudspeaker System Analysis," *J. Audio Eng. Soc*, vol. 20, no. 5, pp. 383–395, 1972.

[11] W. Klippel and U. Seidel, "Fast and accurate measurement of linear transducer parameters," *Prepr. Eng. Soc.*, pp. 1–7, 2001.

[12] F. Silva, J. Kergomard, C. Vergez, and J. Gilbert, "Interaction of reed and acoustic resonator in clarinetlike systems," *J. Acoust. Soc. Am.*, vol. 124, no. 5, pp. 3284–3295, 2008.

[13] V. Gibiat, "Acoustical impedance measurements by the two-microphone-three-calibration (TMTC) method," *J. Acoust. Soc. Am.*, vol. 88, p. 2533, 1990.

[14] A. Chaigne and J. Kergomard, *Acoustique des instruments de musique*. Belin, 2008.

[15] M. Atig, J.-P. Dalmont, and J. Gilbert, "Saturation mechanism in clarinet-like instruments, the effect of the localised non-linear losses," *Appl. Acoust.*, vol. 65, pp. 1133–1154, Dec. 2004.

[16] "Xenomai: Real-Time Framework for Linux." http://www.xenomai.org.

[17] S. Benacchio, R. Piéchaud, and A. Mamou-Mani, "Active Control of String Instruments using Xenomai," in *15th Real Time Linux Work.*, 2013.

A The computing system

The hybrid operation requires a "real-time" feedback-loop that includes a numerical interface. We opted for a cheap solution that concerns the recompilation of a Linux kernel on standard PC architecture, which is covered by the *Xenomai* framework [16]. This system includes special drivers (by the *Analogy* software) that allow for a uninterrupted access to a *National Instruments* 6052E 16-bit acquisition card that provides analogue in- and outputs.

In order to link the generated Simulink C-code to this system, we relied on the work by Benacchio et al., who created a patch that inserts the *Analogy* driver-code into the Simulink code [17].

As such, we could use this system with a minimum sampling time (without overruns) of T_s = 30 µs, corresponding to a sampling rate of f_s = 33 333.3 Hz, which is high enough for our purpose. While a "continuous solver" is not supported (yet), the applied filters and quasi-static mouthpiece model don't hold any continuous states.